New Phytologist

Comprehensive microarray profiling of cell wall related polymers and enzymes in the parasitic plant Cuscuta reflexa and the host Pelargonium zonale

Journal:	*New Phytologist*
Manuscript ID:	Draft
Manuscript Type:	MS - Regular Manuscript
Date Submitted by the Author:	n/a
Complete List of Authors:	Johnsen, Hanne; UiT The Arctic University of Norway, Department of Arctic and Marine Biology Ketelsen, Bernd; UiT The Arctic University of Norway, Department of Arctic and Marine Biology Olsen, Stian; UiT The Arctic University of Norway, Department of Arctic and Marine Biology Vidal-Melgosa, Silvia; University of Copenhagen, Department of Plant and Environmental Sciences Fangel, Jonatan; University of Copenhagen, Department of Plant and Environmental Sciences Willats, William; University of Copenhagen, Department of Plant and Environmental Sciences Krause, Kirsten; UiT The Arctic University of Norway, Department of Arctic and Marine Biology
Key Words:	parasitic plants, Cuscuta, haustoria, cell wall composition, pectin, arabinogalactan proteins

Comprehensive microarray profiling of cell wall related polymers and enzymes in the parasitic plant *Cuscuta reflexa* and the host *Pelargonium zonale*

Hanne Risan Johnsen[1], Bernd Ketelsen[1], Stian Olsen[1], Silvia Vidal-Melgosa[2], Jonatan U. Fangel[2], William G.T. Willats[2] and Kirsten Krause[1]*

[1]Department of Arctic and Marine Biology, Faculty of Biosciences, Fisheries and Economics, UiT The Arctic University of Norway, 9037 Tromsø, Norway

[2]Department of Plant and Environmental Sciences, Faculty of Science, University of Copenhagen, Frederiksberg, Denmark

*corresponding author:
Kirsten Krause
E-Mail: kirsten.krause@uit.no;
Tel.: +47-776-46415
Fax: +47-776-46333

Word count: Total 6.014

(Summary: 186; Introduction: 837; Results: 2181; Discussion: 1193; Material and Methods: 1521; Acknowledgement: 90)

Figures: 7 (Figures 1 to 5 in color)

Tables: 0

Supplementary Information: 3 Tables

Summary

- Host plant penetration by holoparasitic dodder (genus *Cuscuta*) poses an apparent conflict: while hydrolytic enzymes are needed to break down host cell walls, the parasites own walls need to be resistant to enzymatic attack.
- We investigated cell wall composition and enzyme activities at infection sites in the compatible interaction between *Cuscuta reflexa* and the host *Pelargonium zonale* using microarray profiling techniques and immunohistolabeling.
- Crude extracts of *C. reflexa*'s haustoria displayed high pectolytic activity accompanied by accumulation of pectate lyase transcripts. Pectin was detected in the haustoria regardless of their strong pectolytic activity, while in infected hosts evidence for changes in pectin methyl esterification levels at haustorial interfaces were obtained. Esterified pectins were detected in *C. reflexa* by immunohistolabeling, while chemical extraction of cell wall components failed to recover them, indicating differences to host pectin properties. Haustoria also revealed elevated levels of arabinogalactan proteins compared to parasitic stems and host tissues.
- Host pectin de-esterification may pave the way for subsequent pectin breakdown and progression of the haustorium. A mechanism preventing haustorial cell wall degradation by native enzymes may be connected to pectin properties or arabinogalactan protein abundance.

Key Words
Cuscuta, cell wall composition, haustoria, parasitic plants, pectin

Introduction

Cuscuta is a large angiosperm genus comprising approximately 200 species all of which share a parasitic life style. As an adaptation to their lifestyle, leaves and roots have been substantially reduced (Fig.1a). The key event in the evolution of plant/plant parasitism, however, was the invention of specialized multicellular feeding organs called haustoria. With these, some of the more robust *Cuscuta* species such as *Cuscuta reflexa* can attack and kill fruit trees but more commonly thrive on herbaceous hosts or ornamental plants. The parasitic attack is commenced by a twining of the parasite around the stems or petioles of the host and a swelling of shoot areas proximal to the host tissue (Vaughn, 2002). The invasion of host tissue by the haustoria of *Cuscuta* then proceeds rapidly and culminates in the formation of physical and physiological connections between both partners (Christensen et al., 2003; Birschwilks et al., 2006; Albert, 2008). The prerequisite to successful infection is that the parasite can overcome the mechanical barriers of the host plant, mainly the cuticle and the cell walls. Cell walls consist of cellulose microfibrils that are interconnected in a matrix consisting of polysaccharide polymers such as hemicelluloses and pectins (Cosgrove, 2005). They render considerable rigidity to the cells and are rather resistant to perforation or rupturing.

Pectins are the main components of the primary cell wall and middle lamella of dicotyledonous species and are generally grouped into three major types that are covalently linked to form macromolecules in the cell wall: homogalacturonan (HG), rhamnogalacturonan I (RG-I), and the substituted rhamnogalacturonan II (RG-II) (Willats et al., 2001). HG is the most abundant pectic polysaccharide in plant cell walls. It is polymerized in the Golgi apparatus by a number of glycosyl

transferases (Caffall & Mohnen, 2009) and secreted to the cell wall in a highly (70 – 80 %) methyl esterified state where it is subsequently de-esterified by the action of pectin methyl esterases (PMEs) (Pelloux et al., 2007). The de-esterification of pectins by PMEs affects the interaction of pectin with celluloses and xyloglucan (Caffall & Mohnen, 2009) and influences the capacity to form calcium cross-links between pectin fibers, resulting in a strengthening of cell walls (Willats et al., 2001). On the other hand, de-esterification also allows degradation by polygalacturonases (PGs) and pectate lyases (PLs) and can thereby be involved in softening and degradation of the cell wall (Wakabayashi et al., 2003), which plays an important role in the invasion of plant tissues by bacterial and fungal pathogens (Zhang & Staehelin, 1992; Orfila et al., 2001). A subsequent degradation of de-esterified pectins has been shown to facilitate further breakdown of cellulose and hemicelluloses (Lionetti et al., 2010).

In comparison to our vast knowledge on the arsenal of hydrolytic enzymes used by plant parasitizing microbes and fungi to achieve host penetration, the mechanisms of parasitic plant penetration are considerably less researched. The few reports that have been published, meanwhile, point to a combination of mechanical pressure applied to the host tissue and enzymatic modification or degradation of host cell walls by a cocktail of secreted hydrolytic enzymes. Elevated activities of PMEs, PGs, cellulases and peroxidases were recorded in *Cuscuta* spp. (Nagar et al., 1984; Srivastava et al., 1994; Bar Nun & Mayer, 1999; Bar Nun et al., 1999; Lopez-Curto et al., 2006; Johnsen & Krause, 2014) and may help to create fissures in the host stem through which the haustorium can invade. Recently, a cysteine-protease, Cuscutain, has been identified specifically at the surface of haustorial cells (Bleischwitz et al., 2010). Some host plants seem to respond to a

Cuscuta attack by synthesizing proteins that contribute to cell wall elongation, modification and architecture (Werner et al., 2001; Albert et al., 2004).

One of the main questions that remain unanswered is how these parasites manage to direct the action of the assumed hydrolytic cell wall breakdown exclusively towards the host and how they protect their own haustorial cell walls from self-degradation. In order to approach this question, we have used the comprehensive microarray polymer profiling (CoMPP) technique (Moller et al., 2007) and novel glycan microarrays based on epitope depletion by carbohydrate-active enzyme (CAZyme) degrading activities to generate high-density overviews over carbohydrate epitope occurrence and CAZymes, respectively, in the *Pelargonium zonale*/*Cuscuta reflexa* interaction. *P. zonale* (commonly known as geranium or storkbill) is a preferred host to *Cuscuta* spp. and its interaction with the parasite is well characterized by electron microscopical studies (Dorr, 1969; Christensen et al., 2003). Based on the array data and from supporting results from immunohistolabeling of cross sections from the host/parasite interface and RT-qPCR measurements, it is obvious that pectin de-esterification of the host tissue prior to or during infection is crucial for the rapid and effective progression of the haustorium along the middle lamella and may keep cell destruction in the host to a minimum. Simultaneously, the answer to why the haustorium is not degraded by its own lytic arsenal might lie in the parasite's pectin methylation status or in the way it is cross-linked with other molecules in middle lamella of the haustorium.

Results

Cell wall compositional profiling of *Cuscuta reflexa* and *Pelargonium zonale*

The cell wall compositions of *C. reflexa* and *P. zonale* were assessed by the relative levels of 31 cell wall glycan and extensin epitopes detected by a range of cell wall directed monoclonal antibodies (mAbs) and carbohydrate binding modules (CBMs). In addition to plant material of non-infective/non infected stem regions, infection sites were dissected in order to separate parasite and host tissue from one another. While the non-endophytic part of the infection structure (called "adhesive disk" (Dawson, 1994) or "upper haustorium" (Lee, 2007)) can be easily detached by pulling host and parasite apart, the endophytic mature haustorium often remains inside the host and requires removal with a scalpel (Fig. 1c-e). In contrast to the surrounding host tissue, the haustoria were considerably softer and showed pronounced browning when exposed to air for some time. Alcohol Insoluble Residues (AIR) of the different samples were generated and extracted sequentially using CDTA and NaOH (see Material and Methods). CoMPP provides semi-quantitative information about the relative abundance of cell wall polysaccharides, and gives an overview of polymer occurrence via epitope frequency. The results of the analysis are shown in a heat map displaying all the tested mAbs and CBMs (Fig. 2).

As expected, most epitopes detected in the CDTA extracts were related to pectin, while the NaOH extracts mainly contained hemicelluloses and glycoproteins. In general, the cell wall composition of *P. zonale* displayed similarities to the cell walls of tobacco and grapevine leaves that have been recently profiled by the same technique (Nguema-Ona et al., 2012; Moore et al., 2014). Compared to these non-parasitic plants, *C. reflexa* exhibited a

generally higher content of hemicelluloses but otherwise showed a similar composition of the basic cell wall polysaccharides. Significant amounts of homogalacturonan (HG) in extracts from *P. zonale* were detected by a range of mAbs reported to bind to HG epitopes with different degrees of esterification (DE) (mAbs JIM5, JIM7, LM18, LM19, LM20 and 2F4). Most HG epitopes were soluble in CDTA, but the presence of epitopes detected by mAb LM19 at lower levels in the NaOH extracts suggests that a small portion of the HGs are linked to non-cellulosic polysaccharides. The abundance of HG in *C. reflexa* was similar to that of *P. zonale* with one exception: the LM20 epitope representing highly esterified pectins was absent in both extracts from *C. reflexa*. The RG-I backbone recognized by the monoclonal antibodies INRA-RU1 and INRA-RU2 was predominantly found in CDTA extracts from *P. zonale*, although the galactan (mAb LM5) and arabinan (mAb LM6) side chains of RG-I had the highest abundance in the haustoria of *C. reflexa*. Unlike the other pectic epitopes that were only extracted by CDTA, galactan and arabinan were also present in the NaOH extracts (Fig. 2). The presence of galactan and arabinan epitopes in the NaOH extracts together with mannans and xyloglucans indicate an association between the side chains of RG-I and hemicelluloses. These results are consistent with previous findings pointing to a co-occurrence of some glycans by CoMPP analysis (Moller et al., 2007).

Furthermore, xyloglucans (recognized by mAbs LM15, LM24 and LM25) were mainly detected in the NaOH extracts, whereas most of the arabinogalactan proteins (AGPs) appeared to be extracted by CDTA (recognized by mAbs JIM13, JIM14 and LM2). AGPs were particularly abundant in the haustoria of *C. reflexa* (Fig. 2). The solubility of extensins (recognized by mAbs LM1 and JIM20) differed between *C. reflexa* and *P. zonale*. Extensins from *P.*

zonale were exclusively detected in the CDTA extract, while extensins from *C. reflexa* were extracted mainly by NaOH (Fig. 2). The xylogalacturonan epitope (recognized by mAb LM8), previously thought to be restricted to detaching cells or floral organs in a range of angiosperms (Willats et al., 2004; Moller et al., 2007; Zandleven et al., 2007), was detected in both NaOH extracts from *C. reflexa*. Likewise, the epitope recognized by mAb LM16, binding to branched arabinan, was only detected in the haustorial extracts from *C. reflexa*. The binding of BS-400-2, recognizing callose was restricted to the NaOH extracts from the haustoria of *C. reflexa*. These findings corroborate previous immunolocalization studies which reported callose exclusively in association with plasmodesmata along the searching hyphae and at the tips of growing hyphae (Vaughn, 2003).

Cell wall epitope profiles in crude plant extracts

As part of the CAZymes screening by epitope depletion, we generated plant extracts (in 50 mM sodium acetate, 15 mM NaCl, 8% Polyvinylpolypyrrolidone buffer, pH 5.5) from *C. reflexa* and *P. zonale* tissues. Polysaccharides present in these extracts were additionally investigated by printing the crude plant extracts as microarrays. The produced arrays were probed with a wide collection of anti-cell wall probes and binding results are shown in Fig. 3. The heat map results of *C. reflexa* showed some differences compared to the combined AIR extracts (Fig. 2) that can be primarily attributed to the relative insolubility of the corresponding carbohydrate macromolecules in the different used solvents. However, that signals were observed for some epitopes in infected or uninfected hosts but not in *C. reflexa* (despite their strong signals in CDTA extracts, see Fig. 2) could also point to differences in physico-chemical properties or in crosslinking in both plants. For *P. zonale*, an additional sample from infected stem

areas was included in the analysis, which revealed some differences in cell wall composition between infected and uninfected hosts. Infected tissue exhibited a higher degree of pectin with a low DE detected by JIM5 and LM19 (Clausen et al., 2003; Verhertbruggen et al., 2009) in comparison to the non-infected tissue of *P. zonale*. While pectin with a high DE identified by JIM7 and LM20 (Clausen et al., 2003; Verhertbruggen et al., 2009) was hardly detected around the infection sites, it was dominant in the non-infected tissue of *P. zonale*. Detection of the galactan and arabinan side chains of RG-I (recognized by LM5 and LM6, respectively) in uninfected and infected host tissue indicated an increase of these epitopes upon infection. Extensins and callose are known to accumulate in response to wounding to provide a physical barrier against pathogens (Corbin et al., 1987; Kawalleck et al., 1995). In *P. zonale*, however, there was no detectable increase of either extensins (LM3, JIM20) or callose (BS-400-2) following infection by *C. reflexa*. In contrast, several AGP epitopes were detected more strongly in infected hosts than in uninfected hosts. This is consistent with a previous observation reporting increased expression of an AGP at the contact site of *C. reflexa* pre-haustoria on tomato stems early on during infection (Baron-Epel et al., 1988; Albert et al., 2006).

CAZyme activity assessment by epitope depletion in *C. reflexa* and *P. zonale* extracts

The removal or modification of cell wall epitopes as a result of CAZyme activities can be used to analyze plant extracts for cell wall degrading or modifying enzyme activities. A high-throughput immuno-glycoarray method has been developed for that and has been recently used for the screening of CAZyme related activities (Agger et al., 2014). In brief, plant extracts from different *C. reflexa* and *P. zonale* tissues were incubated with three defined

277 polysaccharide mixtures (see Fig. 4, legend) in a microtiter plate.
278 After incubation, the content of the plate was spotted as
279 microarrays and arrays were probed with a wide collection of
280 mAbs and CBMs specific for the polysaccharides present in the
281 substrate mixtures. Decreased antibody binding as a result of the
282 incubation indicates digestion or modification of the corresponding
283 epitopes (Obro et al., 2009; Sorensen et al., 2009) by the extracts.
284 Two commercial enzymes (endo-polygalacturonase and endo-1-3-
285 β-glucanase) were used in control set-ups. The results are
286 presented in a fold change heat map, where average signals from
287 the untreated control are divided by average signals from treated
288 samples (Fig. 4a-c).
289 Incubation of extracts from *C. reflexa* with mixture 1 (containing
290 arabinoxylan, galactomannan, β-glucan and pectin with a DE of
291 81%), revealed enzyme activities mainly against pectin. The
292 reduction in binding was high for JIM7 and LM20 that represent
293 more highly methyl-esterified pectins, and for JIM5, which
294 preferably binds low methylated pectins but also un-esterified and
295 partially methyl-esterified HG with a wide range of DEs (Clausen
296 et al., 2003; Verhertbruggen et al., 2009). Although less
297 pronounced, LM20 and JIM7 also showed a decrease in binding in
298 the infected tissue of the host, compared to no measurable activity
299 in the un-infected host stems (Fig. 4a). The low methyl esterified
300 pectin (lime pectin with a DE of 16%) in mixture 3 (Fig. 4c) was
301 degraded by all extracts having a higher fold change with mAb
302 LM19 (binding to low DE pectins) with stem, pre-haustoria and
303 un-infected host extracts. The same was observed when using
304 polygalacturonan from mixture 2 (Fig. 4b) as substrate. The stem
305 and pre-haustoria extracts also displayed some activity against RG-
306 I, indicated by reduced binding of mAbs INRA-RU1 and INRA-
307 RU2 to mixture 2.

In addition, incubation with extracts from *C. reflexa* but especially from the infected host caused a diminished binding of CBM30 (Fig. 4a-b). This CBM binds to β-1-4-glucopolymers including barley β-glucan (mixture 1) and lichenan (mixture 2) (Arai et al., 2003). The extracts from *C. reflexa* haustoria, moreover, caused a slight decrease in binding of mAb LM11, indicating some activity against the arabinoxylan in mixture 1.

Incubation with extracts from haustoria and infected host diminished binding of mAbs LM15 and LM25 recognizing a specific epitope from the xyloglucan present in mixture 3, whereas extracts from *C. reflexa* stem as well as the un-infected host decreased the binding intensity of another anti-xyloglucan mAb, LM24. Xyloglucans are known to be involved in cell wall elongation and restructuring, a xyloglucan transglycosylase/ hydrolase was shown to be up-regulated in the host upon infection with *C. reflexa*. The response was observed both adjacent to the invasive haustoria, but also as a systemic response in tissues without direct contact to the parasite (Albert et al., 2004).

Gradients of pectin esterification in cells at the host/parasite interface

For the above described analyses homogenized extracts were employed that are limited in their spatial resolution. In order to probe for differences directly at the host/parasite interface, immunofluorescence labeling of cross sections was employed. LM20 labeling was weaker in cell walls adjacent to the penetrating haustoria than in the opposite, distal end of the same cell (Fig. 5). This was particularly evident at the very tip where haustorial growth can be assumed to still be progressing. At the same time, the binding to low methyl esterified pectins recognized by LM19

was stronger in the same areas compared to the distal walls. Generally, LM19 labeled more strongly in the epidermal and cortex layers of the host, while LM20 labeled rather evenly throughout the stem (with exception of tissue directly adjacent to the haustorium). *C. reflexa* showed somewhat weaker labeling with LM20, although fluorescence with this antibody was clearly visible in the endophytic part of the haustorium (Fig. 5), despite the failure of this epitope being detected in any parasitic tissue by CoMPP.

Xyloglucan epitope demasking at the host/parasite interface as indication for pectolytic activity *in situ*

Immunofluorescence-based localization of xyloglucan with mAb LM24 on cross sections of the interface between *C. reflexa* and *P. zonale* revealed a higher signal in areas directly adjacent to the penetrating haustoria (Fig. 6a, b). The haustoria themselves did not show any labeling with LM24. Previous immunolocalisation studies have revealed that xyloglucan, xylan and mannan epitopes can be masked in plant cell walls by the presence of pectin (Marcus et al., 2008; Hervé et al., 2009; Herve et al., 2010), prompting us to check whether the lack of labeling in the haustoria of *C. reflexa* and in the host cells distant from the infection site could be due to pectin-based masking. Enzymatic pre-treatment of cross sections with pectate lyase led to a significant increase in binding by the anti-xyloglucan antibody to cell walls in the host but not in the parasite (Fig. 6c, d). Additionally, immunolabeling with LM21, recognizing mannans, indicate a similar de-masking of mannans in areas adjacent to the haustoria (data not shown). These observations support the notion that the parasite mediates the degradation of pectic polysaccharides at the site of infection, but that the absence of detectable epitopes in the parasite, in return, must have other reasons.

Expression of pectate lyases in *C. reflexa*

In order to examine if PL gene expression in *Cuscuta* is induced in haustorial infection sites, the relative transcript abundances of five genes from *C. reflexa* encoding PLs, Cr-PL-1 to -5, were quantified using RT-qPCR (see Fig. 7). The genes were initially identified by transcriptome sequencing of the parasite (Hollmann et al., unpublished). The transcript abundance of Cr-PL-1 is greatly increased (50-fold change) in the infective tissue compared to the stem. Cr-PL-2, Cr-PL-4 and Cr-PL-5 are also higher expressed in the haustorial tissue, but the differences are not as prominent (6-fold, 4-fold and 3-fold change, respectively). The expression of Cr-PL-3 does not differ substantially between the two tissue types (1.7-fold change). All numerical values can be found in the supplements. In summary, overall pectate lyase expression is enhanced in the infective tissue, with one enzyme in particular that can be linked to this tissue.

Discussion

Parasitic plant haustoria penetrate host plant tissue in order to supply the parasite with host-derived nutrients. Despite their name, parasitic plant haustoria differ from fungal haustoria not only by their multicellularity but also in their ostensible similarity with the tissue that they invade. Being an organ of a higher plant, the parasitic plant haustorium must naturally be confined to the same general cell wall building blocks as the host cell walls. If haustorial progression by parasitic plants is dependent to a large part on enzymatic softening of host cell walls, as is the predominant opinion, then one has to ask how the cell walls of haustorial cells, particularly at the interface to the host, are protected against digestion by their own enzymes.

To test if indeed enzymes secreted by parasitic plants contribute to a measurable change in host cell wall properties, we have investigated infection sites in the compatible interaction between the stem holoparasite *C. reflexa* and the host *P. zonale* using novel high throughput methods like CoMPP and immuno-glycoarrays. We gathered support for our observations by immunohistolabeling of infection sites. Our results corroborate the notion that enzymatic degradation softens the host tissue for an infection and paves the way for the intrusion of the haustorium.

Although the paucity of data addressing the modalities that enable parasitic plants to invade their hosts limits detailed comparisons, some penetration strategies or groups of enzymes seem to be universally used by pathogenic organisms (Mayer, 2006). Among the primary targets of lytic degradation by different pathogens are the pectic polysaccharides in the middle lamella between adjacent cells. Many studies have provided evidence for alteration in host pectinase activity in response to fungal and bacterial pathogen infections, which in turn has been shown to make the cell wall

more prone to degradation (Raiola et al., 2011). Since pectins are known to control the porosity of the cell wall (Baron-Epel et al., 1988), degradation of pectin will increase the availability of substrates targeted by other cell wall degrading enzymes (Cantu et al., 2008; Nuhse, 2012). Not surprisingly, therefore, the possession of pectinolytic enzymes could also be demonstrated in the root parasite *Orobanche* (Losner-Goshen et al., 1998) and the shoot parasite *C. reflexa* (Srivastava et al., 1994; Losner-Goshen et al., 1998; Vaughn, 2003). Increased expression of several cell wall modifying enzymes, among them PMEs and PLs in the infective stages of *C. pentagona* was recently reported (Ranjan et al., 2014). Our own work further corroborates the general notion of pectin degradation being an important determinant during the attack by *Cuscuta*. The ability of PLs and PGs to degrade pectin is dependent of the degree of methyl esterification. Since pectins exist in a highly esterified state after polymerization, de-esterification of the HGs by PMEs is essential for PL- and PG-mediated degradation. The CoMPP data, indeed, showed a profound difference in the overall methyl-esterification levels in uninfected and infected hosts (Fig. 2 and 3). While uninfected hosts appear to abound with highly esterified pectins, infected hosts have higher levels of low esterified pectins. Concomitantly, infected but not uninfected hosts displayed high relative enzyme activities acting on the highly methyl-esterified lime pectin (mixture 1) in the immuno-glycoarrays (Fig. 4a). At the same time, galactan and arabinan side chains of RG-I were detected at increased levels in the host upon infection (Fig. 3). Recent studies have revealed that these side chains can reduce strong interactions between nearby HG chains, preventing crosslinking by means of calcium ions (Jones et al., 2003). The branching of RG-I has mainly been observed in susceptible host plants (Wydra & Berl,

2006). It is quite feasible that they provide a means to secure further degradation by PLs or PGs by preventing newly de-esterified pectins from forming cross-links that would counteract the degradation process.

Gradients of pectin methyl-esterification in the walls of host cells being in direct contact with the haustorial surface (Fig. 5) are congruent with the assumption that the bulk of the PME activity originates directly from the parasite and is diluted with increasing distance from the source cells. This also fits with the elevated expression patterns of corresponding pectin modifying and hydrolyzing genes ((Ranjan et al., 2014) and Fig. 7). However, it cannot be excluded that the parasite in addition causes the host to produce such enzymes, or that their production is part of a natural response pattern of the host to the attack.

Taken alone, our CoMPP data would indicate that highly esterified pectins are missing or depleted in *Cuscuta* (Fig. 2 and 3). This observation stands in stark contrast to the detection of mAb LM20 in haustorial tissue of immunolabelled cross-sections. Although the labeling intensity in the parasite is somewhat lower (Fig. 5), it is undoubtedly specific. The only way this can be explained is by assuming that the highly esterified pectins (in contrast to their counterparts with low esterification content) failed to be extracted properly when preparing the CoMPP extracts or that their concentrations were too low to guarantee detection in the CoMPP assay. It is known that the PME-generated free carboxyl groups predominantly crosslink with each other via calcium bridges when occurring blockwise in developmentally regulated regions. If this happens, gel-like structures are generated that possess enhanced cell adhesion properties and heightened resistance against degradation (Willats et al., 2001; Willats et al., 2006; Lionetti et al., 2012). Instead, the free carboxyl groups left by the action of

pathogen-derived PMEs are typically more randomly distributed and make HGs susceptible to degradation by PLs and PGs (Cantu et al., 2008; Lionetti et al., 2012). It is plausible to assume that the highly esterified pectins are either crosslinked to other cell wall polymers or entrapped in a matrix of e.g. cellulose, which further prevent the recovery in AIR or their extraction from this fraction. More in depth studies will be needed to investigate whether the *Cuscuta* pectin is different in these ways and whether this contributes to shielding the haustorium against its own wall degrading activities.

Another noteworthy observation of our analysis is the high amount of AGPs in *C. reflexa*, particularly in its haustoria (Fig. 2 and 3). Prior to our analysis, Vaughn, (2003) found that the hyphae of *Cuscuta pentagona* contained a very lipophilic AGP (detected by mAb JIM8) in small punctuate structures. Also, one host-derived AGP was implicated to be involved in the host plant/parasitic plant interaction (Albert et al., 2006). Most recently, AGPs were strongly detected in the endophytes of *Rhinanthus minor* haustoria (Pielach, 2013). AGPs appear to be involved in several fundamental developmental processes, amongst others in defense reactions (Vaughn et al., 2007) and in the establishment of beneficial root-microbe interactions (Nguema-Ona et al., 2013). Strikingly, AGPs are also involved in another intrusive growth process typical for angiosperms: the growth of the pollen tube through stigma and style that culminates in the double fertilization of the egg cell. Although the latter process is executed by a single cell and at a much smaller scale, the deposition of AGPs at the pollen tube tips (Pereira et al., 2006; Dardelle et al., 2010) as a prerequisite for pollen tube growth is an intriguing model that may be worth investigating in parasitic plant haustoria, too.

Material and methods

Plants and tissue samples

Cuscuta reflexa was grown in a greenhouse on the compatible host *Pelargonium zonale*. For isolation of haustoria, parasite and host were pulled apart. While this separated the pre-haustoria from the host, the majority of haustoria remained inside the host. From there they were manually extracted with a sharp scalpel (Fig. 1). The remaining infected host tissue was trimmed to remove intermittent non-infected areas and collected for AIR preparation. The level of contamination with the adjoining tissue was very minor. Non-infective *Cuscuta* samples were taken from stem regions several tens of centimeters distant from infection sites while non-infected host tissue was harvested from unattacked shoots of similar diameter as the infected areas.

Alcohol Insoluble Residues (AIR)

Samples were shock-frozen in liquid nitrogen and homogenized using a TissueLyser (Qiagen). Six volumes of 70% ethanol were added to the samples, which were then left to incubate with agitation for 10 min. The insoluble residue was recovered by centrifugation at 6000 rpm and re-extracted five times with ethanol and finally once with 100% acetone. The pellet was air dried and stored at room temperature until analysis.

Comprehensive microarray polymer profiling (CoMPP)

Cell wall glycans were extracted sequentially from the AIRs with the solvents diamino-cyclo-hexane-tetra-acetic-acid (CDTA) and 4 M NaOH following the method described by Moller et al. (Moller et al., 2007; Moller et al., 2012). The extracted material was spotted in triplicate onto sheets of nitrocellulose membrane (Whatman, Maidstone, UK) using a microarray robot with a piezoelectric print head (Sprint, ArrayJet, Roslin, UK). The

resulting arrays were blocked in PBS buffer containing 5% milk powder for 1 hour. Arrays were then probed for 2 hours with a range of mAbs and CBMs (PlantProbes, Leeds, UK; INRA, Nantes, France; BioSupplies, Bundoora, Australia and NZYTech, Lisbon, Portugal) binding to different polysaccharide epitopes, followed by 2 hours incubation with secondary antibodies conjugated to alkaline phosphatase (Sigma, Poole, UK). Antibody binding was detected by 5-bromo-4-chloro-3'-indolyphosphate p-toluidine salt (BCIP) and nitro-blue tetrazolium chloride (NBT). Developed arrays were scanned at 2400 dpi (CanoScan 8800F, Canon, Søborg, Denmark) and converted to TIFFs before binding of probes to individual spots was quantified using microarray analysis software (Array-Pro Analyzer 6.3, Media Cybernetics, Rockville, USA). The results were presented as a heat map (Fig. 2) where the color intensity is proportional to the spot signals. The highest spot signal in the data set is assigned a value of 100 and all other signals adjusted accordingly.

Glycan arrays for the analysis of CAZymes

Plant material from *C. reflexa* and *P. zonale* was frozen in liquid nitrogen, weighed and placed in a mortar with extracting buffer (50 mM sodium acetate, 15 mM NaCl, 8% Polyvinylpolypyrrolidone (PVPP), pH 5.5) in a proportion 1/2 w/v. Once the material was smashed, the mortar content was transferred into an eppendorf tube and stored on ice for 1 hour. Next, the tubes were centrifuged four times at 16000 g at 4 ˚C for 20 minutes (to avoid particles that will block the microarrayer) and last centrifugation supernatants were used for the screening of CAZymes. Defined polysaccharides (purchased from Megazyme International Ireland (Bray, Ireland) except for xylan from Sigma-Aldrich (USA) and lime pectins from DuPont Nutrition Biosciences (Brabrand, Denmark)) were dissolved in dH_2O to a final concentration of 3 mg/ml. Mixtures of

polysaccharides with a final concentration of 0.2 mg/ml per polysaccharide were prepared (see the composition of each mixture in Fig.4 legend) in printing buffer (55.2% glycerol, 44% water, 0.8% Triton X-100). The mixtures of polysaccharides (7.5 µl) were combined with the prepared extracts from *C. reflexa* or *P. zonale* (7.5 µl) in a 384-well microtiter plate having a final volume of 15 µl per well. Controls per each polysaccharide mixture were obtained by combining the mixtures with buffer instead of with extract. Commercial enzymes (Megazyme International Ireland, Bray, Ireland) at a concentration of 2 U/ml were as well included as controls. Each reaction was performed in triplicate. The microtiter plate was covered with Adhesive PCR film (AB-0558, Thermo scientific) to avoid evaporation and subsequently incubated for 2 hours at 30 ˚C and 100 rpm. After incubation, remaining enzymes were inactivated by heating to 80 ˚C for 10 minutes. The content of the plate was spotted as microarrays onto sheets of nitrocellulose membrane with a pore size of 0.45 µm (Whatman, Maidstone, UK) by using a microarray robot (Sprint, Arrayjet, Roslin, UK). The resulting arrays were blocked, probed and quantified as described for CoMPP. Enzyme activity was detected as a decrease in antibody and CBM binding compared to untreated polysaccharide mixtures (controls). The results are presented in a fold change heat map (Fig.4) where the ratio between average signal of the control:average signal of the treated is calculated. Ratios >1 indicate degradation/modification of the epitope recognized by the probe.

Plant extracts polymer profiling.

The same *C. reflexa* and *P. zonale* extracts used for CAZyme analysis were diluted ½ in printing buffer and spotted as microarrays as described above. Probing and quantification was

performed as described for CoMPP and binding results are shown in Fig. 3.

Immunohistolabeling of microtome sections

Sections of 0.5 cm taken from infection sites were collected and directly put into fixative (2 % formaldehyde, 1 % glutaraldehyde in PEM buffer) on ice for 1.5 hours. The fixation was followed by a gradual ethanol dehydration and infiltration with London Resin White® (R1281, Agar Scientific, UK) as described by Hervé et al. (Hervé et al., 2011). Cross sections of 0.5 µm were cut on a microtome using a histo-diamond knife. Resin sections were directly stained with Toluidine Blue O (0.2 % in 1 % Borax solution in water) and mounted in glycerol-based anti-fade mounting medium Citi Fluor AF1 (R1321, Agar) for anatomy studies. For immunohistolabeling, cross sections were incubated for two hours in 1:10 dilutions (in PBS (pH 7.4) + 5 % milk powder) of the primary antibody (LM19 and LM20, PlantProbes, UK) and for 30 minutes in a 1:1000 dilution (in PBS + 5 % milk powder) of the secondary antibody (Alexa Fluor 488, goat anti rat; Invitrogen). Following each incubation step, washing steps with PBS were conducted. Following labelling, the sections were stained with Toluidine Blue O and mounted in glycerol-based anti-fade mounting medium for fluorescence microscopy with a stereo microscope (StereoLumar V12, Zeiss, Germany) or an AxioVert 200M microscope (Zeiss, Germany) equipped with a monochromatic CCD camera (AxioCam HRm Rev. 3; Carl Zeiss).

Pectate lyase treatment and immunohistolabeling of vibratome sections

Fresh mature attachment sites were cut with a VibraTome (Leitz) into 60 µm thick cross sections. When indicated, pectate lyase treatment was conducted prior to immunohistolabeling for 2 hours

631 in 10 µg/ml pectate lyase (Prozomix; 50 mM CAPS (Sigma), 2
632 mM $CaCl_2$) followed by two washing steps of 5 minutes each in
633 PBS. Immunohistolabeling was conducted as described for
634 microtome sections above. After labelling, the sections were
635 mounted on microscope slides and covered with mounting solution
636 (50 % PBS, 50 % glycerol, 0.1 % p-phenylenediamine) and a cover
637 slip. The mounted samples were incubated overnight in darkness at
638 4°C before being analysed by fluorescence light microscopy as
639 described above.

640 **RNA isolation and RT-qPCR**

641 Tissue for RNA isolation was harvested from infective tissue
642 (attachment region detached from host) and stem (5-10 cm distal
643 from infection site) of *C. reflexa* parasitizing *P. zonale* (see Fig. 1).
644 Plant material was snap-frozen in liquid nitrogen and homogenized
645 using a TissueLyser (Qiagen). Total RNA was isolated using a
646 combination of the hot borate method (Wan & Wilkins, 1994) and
647 phenol-chloroform extraction in which pre-warmed (65 °C) borate
648 buffer (200 mM Borax, 30 mM EDTA, 1% (w/v) SDS) and phenol
649 were added to the frozen plant material to make up the first liquid-
650 liquid extraction. Subsequently, one extraction with
651 phenol:chloroform:isoamylalcohol (25:24:1) and two with
652 chloroform:isoamylalcohol (24:1) were executed before total RNA
653 was precipitated in 2M LiCl at 4 °C over night. In order to remove
654 residual gDNA, RNA isolates were treated with DNase using the
655 DNA-free kit (Ambion). Removal of gDNA and integrity of RNA
656 was checked by agarose gel electrophoresis. cDNA was
657 synthesized from 1 µg DNase-treated total RNA using the
658 SuperScript II Reverse Transcriptase (Invitrogen) with anchored
659 Oligo(dT)18 primers. No-reverse transcriptase controls were done
660 for each target gene in order to verify the complete absence of
661 contaminating DNA. Quantitative real-time PCR was performed in

20µl reactions consisting of 10µl SsoFast EvaGreen Supermix (Bio-Rad), 500nM of each primer, 5µl cDNA dilution and nuclease-free water. The CFX96 Real-Time PCR Detection System (Bio-Rad) was used for amplification and fluorescence detection with the following cycling conditions: 95 °C for 30 sec followed by 40 cycles of 95 °C for 5 sec and 61 °C for 5 sec. After 40 cycles, melt curves were recorded by stepwise heating from 65 °C to 95 °C. The efficiency of each amplification reaction (see primer sequences in Supplemental Table S1) was determined by generating standard curves from 10-fold dilutions of cDNA. The differences in PCR efficiencies were taken into account when calculating the relative quantities of each target transcript (Pfaffl, 2001). Relative quantities of Cr-Actin and Cr-SF2 were used to normalize the expression levels between samples. Data were analysed using the CFX Manager Software 2.0 (Bio-Rad).

Acknowledgments

We are indebted to the Phytotron staff in Holt (UiT, Tromsø, Norway), in particular Leidulf Lund, for the caring maintenance of our plants. Coby Weber is thanked for technical assistance in sample preparation and AIR extraction. Prof. Karsten Fischer and Dr. Anna Pielach (UiT, Tromsø, Norway) are thanked for fruitful discussions and critical reading of the manuscript. Funding from Tromsø Forskningsstiftelse (to KK) and from COST FA1006 (for funding of a “short term scientific mission” to HRJ) is gratefully acknowledged. This manuscript is part of the doctoral thesis of HRJ.

References

Agger, J. W., T. Isaksen, A. Várnai, S. Vidal-Melgosa, W. G. T. Willats, R. Ludwig, S. J. Horn, V. G. H. Eijsink and B. Westereng 2014. Discovery of LPMO activity on hemicelluloses shows the importance of oxidative processes in plant cell wall degradation. *Proceedings of the National Academy of Sciences* **111**(17): 6287-6292.

Albert, M., X. Belastegui-Macadam and R. Kaldenhoff 2006. An attack of the plant parasite Cuscuta reflexa induces the expression of attAGP, an attachment protein of the host tomato. *Plant Journal* **48**(4): 548-556.

Albert, M., M. Werner, P. Proksch, S. C. Fry and R. Kaldenhoff 2004. The cell wall-modifying xyloglucan endotransglycosylase/hydrolase LeXTH1 is expressed during the defence reaction of tomato against the plant parasite Cuscuta reflexa. *Plant Biology* **6**(4): 402-407.

Albert, M., X. M. Belastegui-Macadam, et al. 2008. Cuscuta spp: “Parasitic plants in the spotlight of plant physiology". *Economy and Ecology*: 267-277.

Arai, T., R. Araki, A. Tanaka, S. Karita, T. Kimura, K. Sakka and K. Ohmiya 2003. Characterization of a cellulase containing a family 30 carbohydrate-binding module (CBM) derived from Clostridium thermocellum CelJ: Importance of the CBM to cellulose hydrolysis. *Journal of Bacteriology* **185**(2): 504-512.

Bar Nun, N. and A. M. Mayer 1999. Culture of pectin methylesterase and polyphenoloxidase in Cuscuta campestris. *Phytochemistry* **50**(5): 719-727.

Bar Nun, N., A. Mor and A. M. Mayer 1999. A cofactor requirement for polygalacturonase from Cuscuta campestris. *Phytochemistry* **52**(7): 1217-1221.

Baron-Epel, O., P. K. Gharyal and M. Schindler 1988. Pectins as mediators of wall porosity in soybean cells. *Planta* **175**(3): 389-395.

Birschwilks, M., S. Haupt, D. Hofius and S. Neumann 2006. Transfer of phloem-mobile substances from the host plants to the holoparasite Cuscuta sp. *Journal of Experimental Botany* **57**(4): 911-921.

Bleischwitz, M., M. Albert, H. L. Fuchsbauer and R. Kaldenhoff 2010. Significance of Cuscutain, a cysteine protease from Cuscuta reflexa, in host-parasite interactions. *Bmc Plant Biology* **10**.

Caffall, K. H. and D. Mohnen 2009. The structure, function, and biosynthesis of plant cell wall pectic polysaccharides. *Carbohydr Res* **344**(14): 1879-1900.

Cantu, D., A. R. Vicente, J. M. Labavitch, A. B. Bennett and A. L. T. Powell 2008. Strangers in the matrix: plant cell walls and pathogen susceptibility. *Trends in Plant Science* **13**(11): 610-617.

Christensen, N. M., I. Dorr, M. Hansen, T. A. W. van der Kooij and A. Schulz 2003. Development of Cuscuta species on a partially incompatible host: induction of xylem transfer cells. *Protoplasma* **220**(3-4): 131-142.

Clausen, M. H., W. G. Willats and J. P. Knox 2003. Synthetic methyl hexagalacturonate hapten inhibitors of anti-homogalacturonan monoclonal antibodies LM7, JIM5 and JIM7. *Carbohydr Res* **338**(17): 1797-1800.

Corbin, D. R., N. Sauer and C. J. Lamb 1987. Differential Regulation of a Hydroxyproline-Rich Glycoprotein Gene Family in Wounded and Infected Plants. *Molecular and Cellular Biology* **7**(12): 4337-4344.

Cosgrove, D. J. 2005. Growth of the plant cell wall. *Nature Reviews Molecular Cell Biology* **6**(11): 850-861.

Dardelle, F., A. Lehner, Y. Ramdani, M. Bardor, P. Lerouge, A. Driouich and J. C. Mollet 2010. Biochemical and Immunocytological Characterizations of Arabidopsis Pollen Tube Cell Wall. *Plant Physiology* **153**(4): 1563-1576.

Dawson, J. H., L. J. Musselman, P. Wolswinkel, and I. Dörr 1994. Biology and control of Cuscuta. *Reviews of Weed Science*(6): 265-317.

Dorr, I. 1969. Fine Structure of Intracellular Growing Cuscuta-Hyphae. *Protoplasma* **67**(2-3): 123-137.

Hervé, C., S. Marcus and J. P. Knox 2011. Monoclonal Antibodies, Carbohydrate-Binding Modules, and the Detection of Polysaccharides in Plant Cell Walls. *The Plant Cell Wall*. Z. A. Popper, Humana Press. **715:** 103-113.

Herve, C., A. Rogowski, A. W. Blake, S. E. Marcus, H. J. Gilbert and J. P. Knox 2010. Carbohydrate-binding modules promote the enzymatic deconstruction of intact plant cell walls by targeting and proximity effects. *Proceedings of the National Academy of Sciences of the United States of America* **107**(34): 15293-15298.

Hervé, C., A. Rogowski, H. J. Gilbert and J. Paul Knox 2009. Enzymatic treatments reveal differential capacities for xylan recognition and degradation in primary and secondary plant cell walls. *The Plant Journal* **58**(3): 413-422.

Johnsen, H. and K. Krause 2014. Cellulase Activity Screening Using Pure Carboxymethylcellulose: Application to Soluble Cellulolytic Samples and to Plant Tissue Prints.

International Journal of Molecular Sciences **15**(1): 830-838.

Jones, L., J. L. Milne, D. Ashford and S. J. McQueen-Mason 2003. Cell wall arabinan is essential for guard cell function. *Proceedings of the National Academy of Sciences of the United States of America* **100**(20): 11783-11788.

Kawalleck, P., E. Schmelzer, K. Hahlbrock and I. E. Somssich 1995. Two pathogen-responsive genes in parsley encode a tyrosine-rich hydroxyproline-rich glycoprotein (hrgp) and an anionic peroxidase. *Molecular Genetics and Genomics* **247**(4): 444-452.

Lee, K. B. 2007. Structure and development of the upper haustorium in the parasitic flowering plant Cuscuta japonica (Convolvulaceae). *American Journal of Botany* **94**(5): 737-745.

Lionetti, V., F. Cervone and D. Bellincampi 2012. Methyl esterification of pectin plays a role during plant-pathogen interactions and affects plant resistance to diseases. *Journal of Plant Physiology* **169**(16): 1623-1630.

Lionetti, V., F. Francocci, S. Ferrari, C. Volpi, D. Bellincampi, R. Galletti, R. D'Ovidio, G. De Lorenzo and F. Cervone 2010. Engineering the cell wall by reducing de-methyl-esterified homogalacturonan improves saccharification of plant tissues for bioconversion. *Proceedings of the National Academy of Sciences of the United States of America* **107**(2): 616-621.

Lopez-Curto, L., J. Marquez-Guzman and D. M. Diaz-Pontones 2006. Invasion of Coffea arabica (Linn.) by Cuscuta jalapensis (Schlecht): in situ activity of peroxidase. *Environmental and Experimental Botany* **56**(2): 127-135.

Losner-Goshen, D., V. H. Portnoy, A. M. Mayer and D. M. Joel 1998. Pectolytic activity by the haustorium of the parasitic plant Orobanche L. (Orobanchaceae) in host roots. *Annals of Botany* **81**(2): 319-326.

Marcus, S. E., Y. Verhertbruggen, C. Herve, J. J. Ordaz-Ortiz, V. Farkas, H. L. Pedersen, W. G. T. Willats and J. P. Knox 2008. Pectic homogalacturonan masks abundant sets of xyloglucan epitopes in plant cell walls. *Bmc Plant Biology* **8**.

Mayer, A. M. 2006. Pathogenesis by fungi and by parasitic plants: Similarities and differences. *Phytoparasitica* **34**(1): 3-16.

Moller, I., I. Sørensen, A. J. Bernal, C. Blaukopf, K. Lee, J. Øbro, F. Pettolino, A. Roberts, J. D. Mikkelsen, J. P. Knox, et al. 2007. High-throughput mapping of cell-wall polymers within and between plants using novel microarrays. *The Plant Journal* **50**(6): 1118-1128.

Moller, I. E., F. A. Pettolino, C. Hart, E. R. Lampugnani, W. G. T. Willats and A. Bacic 2012. Glycan Profiling of Plant Cell Wall Polymers using Microarrays. *Journal of Visualized Experiments*(70): e4238.

Moore, J. P., E. Nguema-Ona, J. U. Fangel, W. G. T. Willats, A. Hugo and M. A. Vivier 2014. Profiling the main cell wall polysaccharides of grapevine leaves using high-throughput and fractionation methods. *Carbohydrate Polymers* **99**(0): 190-198.

Nagar, R., M. Singh and G. G. Sanwal 1984. Cell-Wall Degrading Enzymes in Cuscuta-Reflexa and Its Hosts. *Journal of Experimental Botany* **35**(157): 1104-1112.

Nguema-Ona, E., J. P. Moore, A. Fagerstrom, J. U. Fangel, W. G. T. Willats, A. Hugo and M. A. Vivier 2012. Profiling the main cell wall polysaccharides of tobacco leaves using high-throughput and fractionation techniques. *Carbohydrate Polymers* **88**(3): 939-949.

Nguema-Ona, E., M. Vicre-Gibouin, M. A. Cannesan and A. Driouich 2013. Arabinogalactan proteins in root-microbe interactions. *Trends in Plant Science* **18**(8): 440-449.

Nuhse, T. S. 2012. Cell wall integrity signaling and innate immunity in plants. *Frontiers in Plant Science* **3**.

Obro, J., T. Sorensen, P. Derkx, C. T. Madsen, M. Drews, M. Willer, J. D. Mikkelsen and W. G. T. Willats 2009. High-throughput screening of Erwinia chrysanthemi pectin methylesterase variants using carbohydrate microarrays. *Proteomics* **9**(7): 1861-1868.

Orfila, C., G. B. Seymour, W. G. T. Willats, I. M. Huxham, M. C. Jarvis, C. J. Dover, A. J. Thompson and J. P. Knox 2001. Altered middle lamella homogalacturonan and disrupted deposition of (1 -> 5)-alpha-L-arabinan in the pericarp of Cnr, a ripening mutant of tomato. *Plant Physiology* **126**(1): 210-221.

Pelloux, J., C. Rusterucci and E. J. Mellerowicz 2007. New insights into pectin methylesterase structure and function. *Trends in Plant Science* **12**(6): 267-277.

Pereira, L. G., S. Coimbra, H. Oliveira, L. Monteiro and M. Sottomayor 2006. Expression of arabinogalactan protein genes in pollen tubes of Arabidopsis thaliana. *Planta* **223**(2): 374-380.

Pfaffl, M. W. 2001. A new mathematical model for relative quantification in real-time RT-PCR. *Nucleic acids research* **29**(9): e45.

Pielach, A. 2013. *Cell wall immunocytochemistry and histology of hemiparasitism in Rhinanthus minor L. and Odontites vernus (Bellardi) Dumort: interactions at haustorial*

interfaces and implications for grassland biodiversity. PhD thesis, National University of Ireland, Galway.

Raiola, A., V. Lionetti, I. Elmaghraby, P. Immerzeel, E. J. Mellerowicz, G. Salvi, F. Cervone and D. Bellincampi 2011. Pectin Methylesterase Is Induced in Arabidopsis upon Infection and Is Necessary for a Successful Colonization by Necrotrophic Pathogens. *Molecular Plant-Microbe Interactions* **24**(4): 432-440.

Ranjan, A., Y. Ichihashi, M. Farhi, K. Zumstein, B. Townsley, R. David-Schwartz and N. R. Sinha 2014. De novo assembly and characterization of the transcriptome of the parasitic weed Cuscuta pentagona identifies genes associated with plant parasitism. *Plant Physiology*.

Sorensen, I., H. L. Pedersen and W. G. T. Willats 2009. An array of possibilities for pectin. *Carbohydr Res* **344**(14): 1872-1878.

Srivastava, S., A. Nighojkar and A. Kumar 1994. Multiple Forms of Pectin Methylesterase from Cuscuta-Reflexa Filaments. *Phytochemistry* **37**(5): 1233-1236.

Vaughn, K. C. 2002. Attachment of the parasitic weed dodder to the host. *Protoplasma* **219**(3-4): 227-237.

Vaughn, K. C. 2003. Dodder hyphae invade the host: a structural and immunocytochemical characterization. *Protoplasma* **220**(3-4): 189-200.

Vaughn, K. C., M. J. Talbot, C. E. Offler and D. W. McCurdy 2007. Wall ingrowths in epidermal transfer cells of Vicia faba cotyledons are modified primary walls marked by localized accumulations of arabinogalactan proteins. *Plant and Cell Physiology* **48**(1): 159-168.

Verhertbruggen, Y., S. E. Marcus, A. Haeger, J. J. Ordaz-Ortiz and J. P. Knox 2009. An extended set of monoclonal antibodies to pectic homogalacturonan. *Carbohydr Res* **344**(14): 1858-1862.

Wakabayashi, K., T. Hoson and D. J. Huber 2003. Methyl de-esterification as a major factor regulating the extent of pectin depolymerization during fruit ripening: a comparison of the action of avocado (Persea americana) and tomato (Lycopersicon esculentum) polygalacturonases. *Journal of Plant Physiology* **160**(6): 667-673.

Wan, C. Y. and T. A. Wilkins 1994. A Modified Hot Borate Method Significantly Enhances the Yield of High-Quality Rna from Cotton (Gossypium-Hirsutum L). *Analytical Biochemistry* **223**(1): 7-12.

Werner, M., N. Uehlein, P. Proksch and R. Kaldenhoff 2001. Characterization of two tomato aquaporins and expression

during the incompatible interaction of tomato with the plant parasite Cuscuta reflexa. *Planta* **213**(4): 550-555.

Willats, W. G. T., P. Knox and J. D. Mikkelsen 2006. Pectin: new insights into an old polymer are starting to gel. *Trends in Food Science & Technology* **17**(3): 97-104.

Willats, W. G. T., L. McCartney, W. Mackie and J. P. Knox 2001. Pectin: cell biology and prospects for functional analysis. *Plant Molecular Biology* **47**(1-2): 9-27.

Willats, W. G. T., L. McCartney, C. G. Steele-King, S. E. Marcus, A. Mort, M. Huisman, G. J. van Alebeek, H. A. Schols, A. G. J. Voragen, A. Le Goff, et al. 2004. A xylogalacturonan epitope is specifically associated with plant cell detachment. *Planta* **218**(4): 673-681.

Willats, W. G. T., C. Orfila, G. Limberg, H. C. Buchholt, G. J. W. M. van Alebeek, A. G. J. Voragen, S. E. Marcus, T. M. I. E. Christensen, J. D. Mikkelsen, B. S. Murray, et al. 2001. Modulation of the degree and pattern of methyl-esterification of pectic homogalacturonan in plant cell walls - Implications for pectin methyl esterase action, matrix properties, and cell adhesion. *Journal of Biological Chemistry* **276**(22): 19404-19413.

Wydra, K. and H. Berl 2006. Structural changes of homogalacturonan, rhamnogalacturonan I and arabinogalactan protein in xylem cell walls of tomato genotypes in reaction to Ralstonia solanacearum. *Physiological and Molecular Plant Pathology* **68**(1-3): 41-50.

Zandleven, J., S. O. Sorensen, J. Harholt, G. Beldman, H. A. Schols, H. V. Scheller and A. J. Voragen 2007. Xylogalacturonan exists in cell walls from various tissues of Arabidopsis thaliana. *Phytochemistry* **68**(8): 1219-1226.

Zhang, G. F. and L. A. Staehelin 1992. Functional Compartmentation of the Golgi-Apparatus of Plant-Cells - Immunocytochemical Analysis of High-Pressure Frozen-Substituted and Freeze-Substituted Sycamore Maple Suspension-Culture Cells. *Plant Physiology* **99**(3): 1070-1083.

964 ## Figure legends

965 **Figure 1. Haustorial parasitism by *Cuscuta*.** (a) Habitus of *C.*
966 *reflexa* [Cr] on *P. zonale* [Pz]. White arrows mark infection sites.
967 (b) Cross section through an infection site. The haustorium [H] in
968 (b) is marked by an arrow. (c-e) Endophytic mature haustoria were
969 removed from *P. zon*ale (Pz) with a sharp scalpel using a
970 stereomicroscope. Scalebars in c to e represent 2 mm.

971 **Figure 2. Comprehensive microarray polymer profiling**
972 **analysis of AIR extracts from *C. reflexa* and *P. zonale*.** The heat
973 map depicts the relative abundance of 31 glycan epitopes in CDTA
974 and NaOH extracts. Specifications and associated epitopes for
975 mAbs and CBMs are given on top. The color intensity in the heat
976 map is proportional to mean spot signals of three replicates. The
977 highest mean spot signal value in the data set was set to 100 and all
978 other values were normalized to this value.

979 **Figure 3. Polysaccharide profiling of plant extracts produced**
980 **for CAZyme analysis.**
981 Heat map depicting the relative abundance of 33 glycan epitopes
982 detected in crude plant extracts from different *C. reflexa* and *P.*
983 *zonale* tissues. Name and associated epitopes for mAbs and CBMs
984 are given on top. Specific plant tissues from which the extracts
985 were generated are listed at the left side of the heat map. The
986 highest mean spot signal value in the data set was set to 100 and all
987 other values adjusted accordingly. Color intensity is proportional
988 to mean spot signals of three replicates.

989 **Figure 4. Carbohydrate-active enzymes activity screening in**
990 **crude plant extracts by epitope depletion.**
991 Plant extracts from *C. reflexa* and *P. zonale* as well as some
992 commercial enzymes (depicted at heat maps left side) were
993 incubated with three polysaccharide mixtures (m1, m2 and m3).
994 Digestion mixtures were printed as microarrays and probed with a

large collection of cell wall related probes. The highest mean spot signal value in the data set was set to 100 and all other values were normalized accordingly. Enzyme activity results are presented in fold change heat maps showing the effect on probes binding to the polysaccharides present in the mixtures. Ratios show average signal of the untreated (control): average signal of the treated. Ratios >1 indicate degradation/modification of the epitope recognized by the probe. Mixture 1 (m1): Pectin DE=81% (lime) + Arabinoxylan (wheat flour) + Galactomannan (carob) + β-glucan (barley), Mixture 2 (m2): Arabinan (sugar beet) + Lichenan (1→3)(1→4)-β-glucan (icelandic moss) + Polygalacturonan (citrus pectin) + Xylan (beechwood) and Mixture 3 (m3): Pectin DE=16% (lime) + Xyloglucan (tamarind) + 2-hydroxyethyl cellulose + Glucomannan (konjac).

Figure 5. Analysis of pectin methyl esterification in infection sites by immunohistolabeling. (a) Overview of a TBO-stained semi-thin section of an infection site of *C. reflexa* (Cr) on *P. zonale* (Pz). Tissue belonging to the parasite (Cr) was colored grey-green for ease of reference. Some parts of the extended hyphae appear unconnected to the main body of the haustorium, this is due to growth outside the z-axis of the cross section. (b, c) Immunofluorescence micrographs of the area shown in (a) after labelling with mAb LM19 and mAb LM20. (d – f) Close-up micrographs of one host cell (*) at the interface with the haustorium. TBO- stain and fluorescence images of the same region are shown. (g – i) Close-up micrographs of two intrusive hyphal cells (*) showing differential staining with mAbs LM19 and LM20, respectively. Scalebars represent 200 µM in a and 20 µM in d and g.

Figure 6. De-masking of host xyloglucan at the parasite/host interface.

(a) Vibratome cross-section showing a portion of an infection site. The border between *C. reflexa* (Cr) and host *P. zonale* (Pz) is marked by a broken line. (b) Micrograph of the same section showing immunofluorescence after labeling with the xyloglucan-specific mAb LM24. (c) Cross-section showing a portion of an infection site after pre-treatment with pectate lyase. (d) Fluorograph of the same section after immunolabeling with mAb LM24. (e, f) Negative controls in which untreated (e) or pectate lyase-treated (f) cross-sections were incubated only with the secondary antibody. Tissue abbreviations: co: cortex, h: haustorium, pth: pith, scl: sclerenchyma. Each scale bar represents 100 µm.

Figure 7. Expression analysis of five pectate lyase genes in stem and infective tissue of *C. reflexa* by RT-qPCR. Columns represent the relative normalized transcript abundances in infective tissue and stem (set to 1). Values are means of three biological replicates plus/minus the standard error of the mean (SEM). Reference genes used for normalization were Cr-Actin and Cr-SF2.

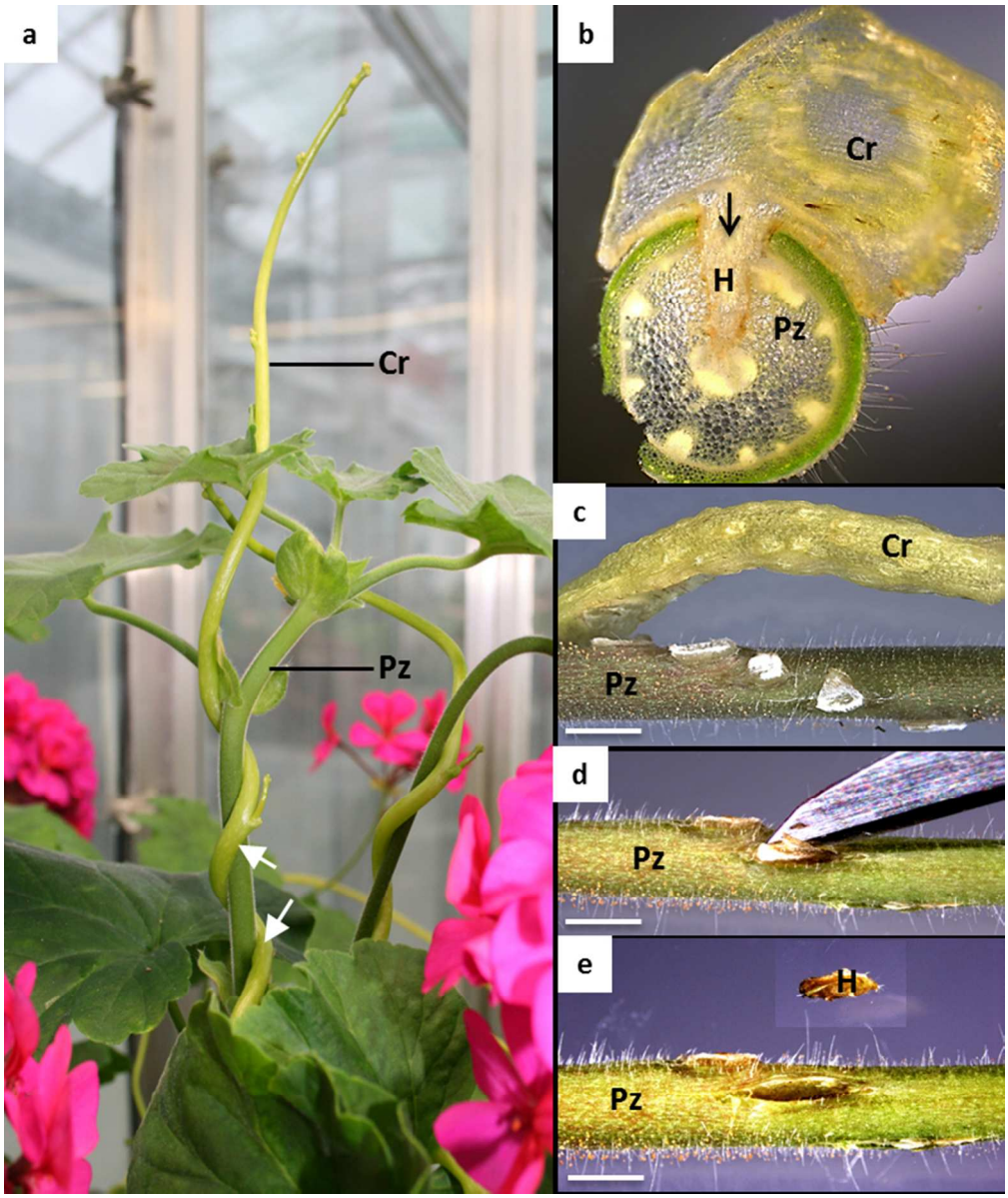

Figure 1. Haustorial parasitism by Cuscuta. (a) Habitus of C. reflexa [Cr] on P. zonale [Pz]. White arrows mark infection sites. (b) Cross section through an infection site. The haustorium [H] in (b) is marked by an arrow. (c-e) Endophytic mature haustoria were removed from P. zonale (Pz) with a sharp scalpel using a stereomicroscope. Scalebars in c to e represent 2 mm.
134x159mm (150 x 150 DPI)

Figure 2

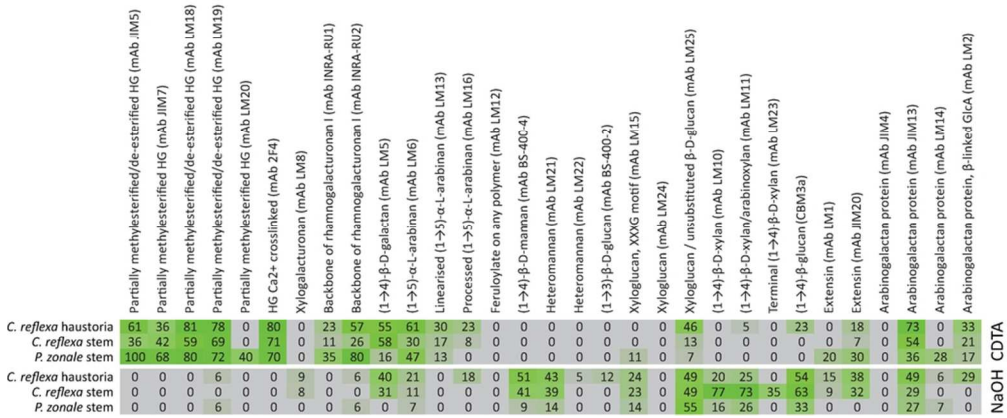

Figure 2. Comprehensive microarray polymer profiling analysis of AIR extracts from C. reflexa and P. zonale. The heat map depicts the relative abundance of 31 glycan epitopes in CDTA and NaOH extracts. Specifications and associated epitopes for mAbs and CBMs are given on top. The color intensity in the heat map is proportional to mean spot signals of three replicates. The highest mean spot signal value in the data set was set to 100 and all other values were normalized to this value.
87x49mm (300 x 300 DPI)

Figure 3

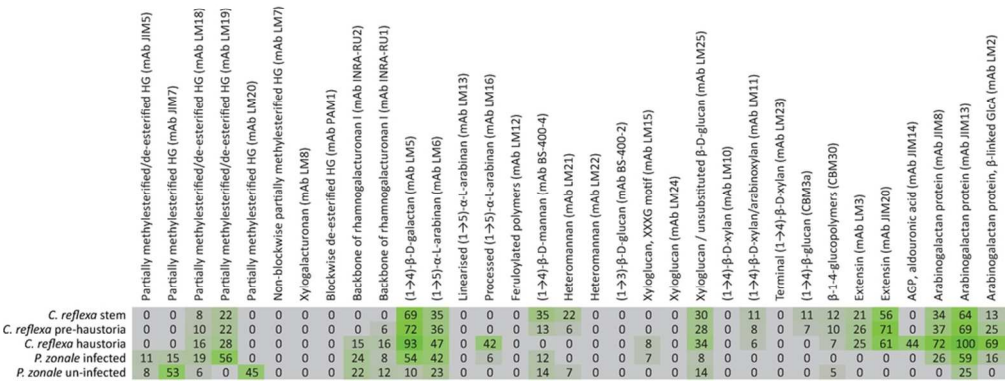

	Partially methylesterified/de-esterified HG (mAb JIM5)	Partially methylesterified HG (mAb JIM7)	Partially methylesterified/de-esterified HG (mAb LM18)	Partially methylesterified/de-esterified HG (mAb LM19)	Partially methylesterified HG (mAb LM20)	Non-blockwise partially methylesterified HG (mAb LM7)	Xylogalacturonan (mAb LM8)	Blockwise de-esterified HG (mAb PAM1)	Backbone of rhamnogalacturonan I (mAb INRA-RU2)	Backbone of rhamnogalacturonan I (mAb INRA-RU1)	(1→4)-β-D-galactan (mAb LM5)	(1→5)-α-L-arabinan (mAb LM6)	Linearised (1→5)-α-L-arabinan (mAb LM13)	Processed (1→5)-α-L-arabinan (mAb LM16)	Feruloylated polymers (mAb LM12)	(1→4)-β-D-mannan (mAb BS-400-4)	Heteromannan (mAb LM21)	Heteromannan (mAb LM22)	(1→3)-β-D-glucan (mAb BS-400-2)	Xyloglucan, XXXG motif (mAb LM15)	Xyloglucan (mAb LM24)	Xyloglucan / unsubstituted β-D-glucan (mAb LM25)	(1→4)-β-D-xylan (mAb LM10)	(1→4)-β-D-xylan/arabinoxylan (mAb LM11)	Terminal (1→4)-β-D-xylan (mAb LM23)	(1→4)-β-glucan (CBM3a)	β-1-4-glucopolymers (CBM30)	Extensin (mAb LM3)	Extensin (mAb JIM20)	AGP, aldouronic acid (mAb JIM14)	Arabinogalactan protein (mAb JIM8)	Arabinogalactan protein (mAb JIM13)	Arabinogalactan protein, β-linked GlcA (mAb LM2)
C. reflexa stem	0	0	8	22	0	0	0	0	0	0	69	35	0	0	0	35	22	0	0	0	0	30	0	11	0	11	12	21	56	0	34	64	13
C. reflexa pre-haustoria	0	0	10	22	0	0	0	0	0	6	72	36	0	0	0	13	6	0	0	0	0	28	0	8	0	7	10	26	71	0	37	69	25
C. reflexa haustoria	0	0	16	28	0	0	0	0	15	16	93	47	0	42	0	0	0	0	0	8	0	34	0	6	0	0	7	25	61	44	72	100	69
P. zonale infected	11	15	19	56	0	0	0	0	24	8	54	42	0	6	0	12	0	0	0	7	0	8	0	0	0	0	0	0	0	0	26	59	16
P. zonale un-infected	8	53	6	0	45	0	0	0	22	12	10	23	0	0	0	14	7	0	0	0	0	14	0	0	0	0	5	0	0	0	0	25	0

Figure 3. Polysaccharide profiling of plant extracts produced for CAZyme analysis.
Heat map depicting the relative abundance of 33 glycan epitopes detected in crude plant extracts from different C. reflexa and P. zonale tissues. Name and associated epitopes for mAbs and CBMs are given on top. Specific plant tissues from which the extracts were generated are listed at the left side of the heat map. The highest mean spot signal value in the data set was set to 100 and all other values adjusted accordingly. Color intensity is proportional to mean spot signals of three replicates.
90x50mm (300 x 300 DPI)

Figure 4

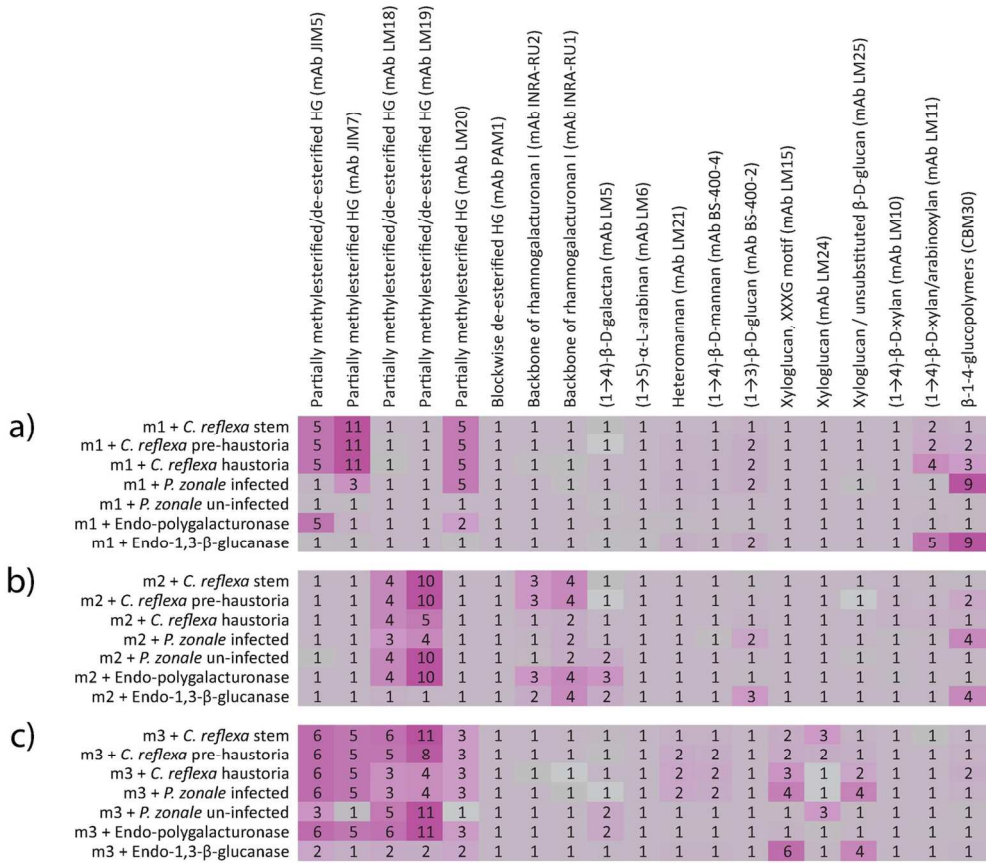

Figure 4. Carbohydrate-active enzymes activity screening in crude plant extracts by epitope depletion. Plant extracts from C. reflexa and P. zonale as well as some commercial enzymes (depicted at heat maps left side) were incubated with three polysaccharide mixtures (m1, m2 and m3). Digestion mixtures were printed as microarrays and probed with a large collection of cell wall related probes. The highest mean spot signal value in the data set was set to 100 and all other values were normalized accordingly. Enzyme activity results are presented in fold change heat maps showing the effect on probes binding to the polysaccharides present in the mixtures. Ratios show average signal of the untreated (control): average signal of the treated. Ratios >1 indicate degradation/modification of the epitope recognized by the probe. Mixture 1 (m1): Pectin DE=81% (lime) + Arabinoxylan (wheat flour) + Galactomannan (carob) + β-glucan (barley), Mixture 2 (m2): Arabinan (sugar beet) + Lichenan (1→3)(1→4)-β-glucan (icelandic moss) + Polygalacturonan (citrus pectin) + Xylan (beechwood) and Mixture 3 (m3): Pectin DE=16% (lime) + Xyloglucan (tamarind) + 2-hydroxyethyl cellulose + Glucomannan (konjac).
126x135mm (300 x 300 DPI)

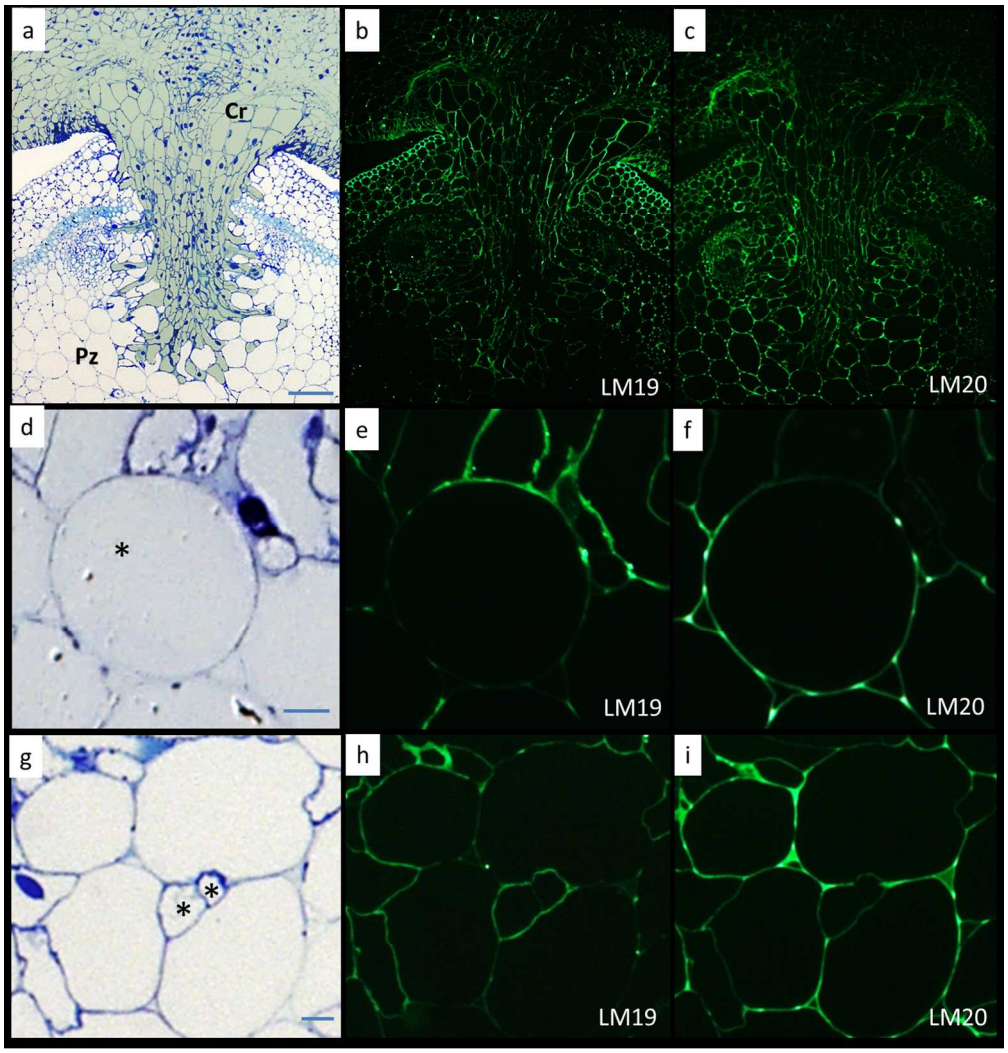

Figure 5. Analysis of pectin methyl esterification in infection sites by immunohistolabeling. (a) Overview of a TBO-stained semi-thin section of an infection site of C. reflexa (Cr) on P. zonale (Pz). Tissue belonging to the parasite (Cr) was colored grey-green for ease of reference. Some parts of the extended hyphae appear unconnected to the main body of the haustorium, this is due to growth outside the z-axis of the cross section. (b, c) Immunofluorescence micrographs of the area shown in (a) after labelling with mAb LM19 and mAb LM20. (d – f) Close-up micrographs of one host cell (*) at the interface with the haustorium. TBO-stain and fluorescence images of the same region are shown. (g – i) Close-up micrographs of two intrusive hyphal cells (*) showing differential staining with mAbs LM19 and LM20, respectively. Scalebars represent 200 µM in a and 20 µM in d and g.
246x257mm (150 x 150 DPI)

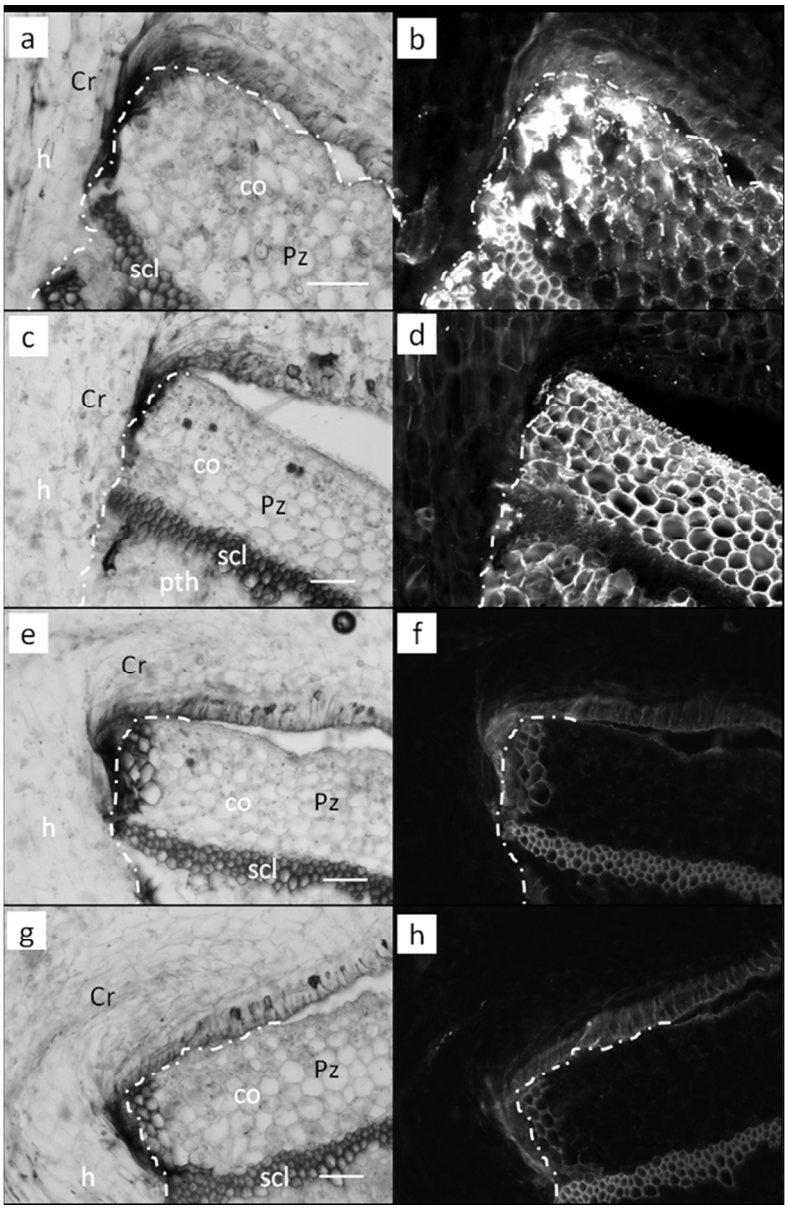

Figure 6. De-masking of host xyloglucan at the parasite/host interface.
(a) Vibratome cross-section showing a portion of an infection site. The border between C. reflexa (Cr) and host P. zonale (Pz) is marked by a broken line. (b) Micrograph of the same section showing immunofluorescence after labeling with the xyloglucan-specific mAb LM24. (c) Cross-section showing a portion of an infection site after pre-treatment with pectate lyase. (d) Fluorograph of the same section after immunolabeling with mAb LM24. (e, f) Negative controls in which untreated (e) or pectate lyase-treated (f) cross-sections were incubated only with the secondary antibody. Tissue abbreviations: co: cortex, h: haustorium, pth: pith, scl: sclerenchyma. Each scale bar represents 100 µm.
124x190mm (150 x 150 DPI)

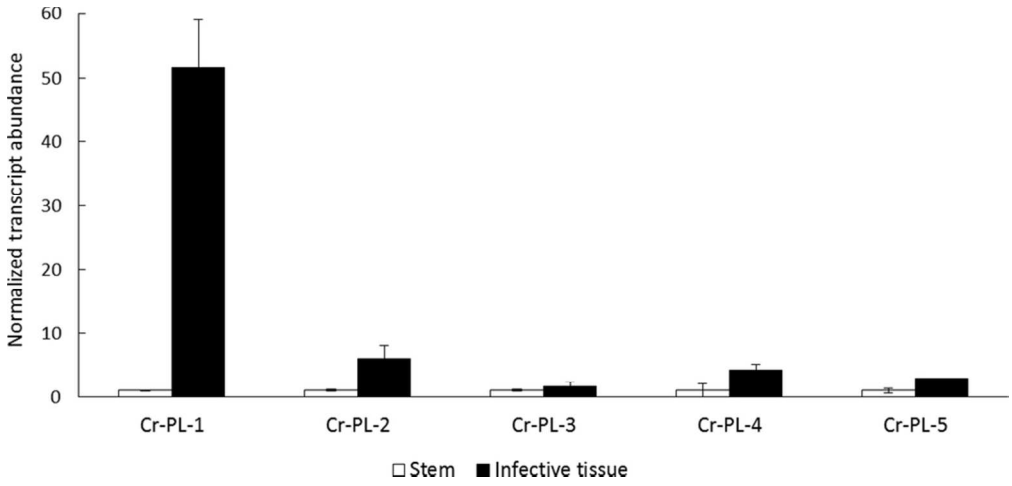

Figure 7. Expression analysis of five pectate lyase genes in stem and infective tissue of C. reflexa by RT-qPCR. Columns represent the relative normalized transcript abundances in infective tissue and stem (set to 1). Values are means of three biological replicates plus/minus the standard error of the mean (SEM). Reference genes used for normalization were Cr-Actin and Cr-SF2.
83x39mm (300 x 300 DPI)